UPDATING THE IMPEDANCE BUDGET FOR ELETTRA 2.0

S. Dastan*, S. Cleva , E. Karantzoulis, S. Krecic, K. Manukyan
Elettra-Sincrotrone Trieste S.C.p.A., Trieste, Italy

Abstract

Elettra 2.0 is a diffraction-limited upgrade of the Elettra storage ring, where beam stability requires an accurate evaluation of the machine impedance. In this work, an updated impedance budget is presented including key vacuum chamber components such as flanges, beam position monitors (BPMs), the scraper system, and resistive wall (RW) effects. Numerical simulations performed with CST Studio Suite and WAKIS are benchmarked against analytical and semi-analytical models. Good agreement is found among the different approaches, providing increased confidence in the updated impedance model and supporting ongoing beam dynamics studies for Elettra 2.0.

INTRODUCTION

The upgrade of Elettra to a diffraction-limited storage ring, described in the Elettra 2.0 Technical Design Report (TDR) [1] and related design studies [2], imposes stringent requirements on beam stability and collective effects. This work presents an updated impedance budget based on detailed numerical simulations and analytical models for selected vacuum chamber components. All calculations assume a Gaussian bunch with rms length σ_z = 4–4.5 mm, corresponding to operation with the third-harmonic cavity (3HC).

SCRAPER IMPEDANCE STUDY

The scraper system considered in this study consists of two cylindrical rods mounted symmetrically with respect to the beam axis inside a rhomboidal vacuum chamber, as shown in Fig. 1. Previous measurements performed on the Elettra scraper system already indicated that the scraper can represent a significant localized impedance source [3], motivating the more detailed analysis presented here. The reference scraper assembly has a total longitudinal length of 93 mm, with the rods positioned at the longitudinal center of the structure and aligned parallel to the beam direction. The surrounding vacuum chamber has a rhomboidal cross section with full horizontal and vertical dimensions of 27 mm and 17 mm, respectively.

In the baseline configuration adopted for the Elettra 2.0 scraper, the rod diameter is D = 13 mm, and the rods can be inserted symmetrically down to a minimum full gap of g = 3 mm. A parametric study was carried out to evaluate the influence of the rod diameter on the longitudinal loss factor. For the Elettra 2.0 geometry, D [Fig. 1(a)] was varied in the range 1–15 mm. The results showed a non-monotonic behavior, with the loss factor increasing up to about D = 5 mm and decreasing for larger diameters, indicating that reducing the rod diameter does not necessarily lead to lower impedance. This behavior suggests that, in addition to the rod diameter, other geometric features—such as the transition between the rods and the vacuum chamber (step) and the overall asymmetry of the structure—also play a significant role in determining the impedance.

Based on these considerations and technical constraints, a rod diameter of D = 13 mm was selected for the final Elettra 2.0 scraper design. The figure provides a schematic view of the main geometric parameters, while the electromagnetic simulations are performed using the full CAD model imported via STL files in order to reproduce the real mechanical design as accurately as possible.

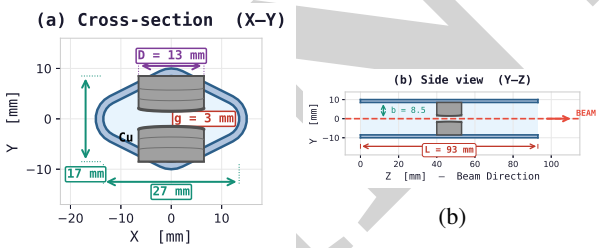

(a) (b)

Figure 1: Schematic geometry of the Elettra 2.0 scraper: (a) transverse cross-section showing the rhomboidal vacuum chamber and cylindrical rods, and (b) longitudinal view along the beam direction. The main geometric parameters are indicated, including the scraper gap g, chamber dimensions, and rod diameter D.

In addition to the geometrical considerations, the numerical results are compared with analytical expressions for short iris-like aperture transitions in the optical regime [4]. In the optical regime, the longitudinal impedance for a rectangular geometry can be expressed as:

$$Z_{\parallel}^{\mathrm{rect}} = \frac{8}{c}\int_0^{\infty} \frac{\sin(\pi a)\cosh(\pi x)}{\cos(2\pi a) - \cosh(2\pi x)} \times \ln\left(\frac{\cosh(\pi x) - \cos(\pi a)}{\cosh(\pi x) + \cos(\pi a)}\right) dx \tag{1}$$

where $a = g/b$ is the ratio between the scraper half-gap and the chamber half-aperture. The corresponding longitudinal loss factor for a Gaussian bunch of rms length σ_z is given by [5]

$$k_{\parallel} = \frac{c}{2\sqrt{\pi}\sigma_z} Z_{\parallel}. \tag{2}$$

The analytical expressions are derived in Gaussian units and are converted to MKS units by multiplying by the factor $cZ_0/(4\pi)$. Using these expressions, the analytical loss

* sara.dastan@elettra.eu

factor was evaluated for different scraper full gaps and compared with the numerical results obtained from Wakis [6] simulations and CST [7] . The comparison is summarized in Table 1.

Table 1: Comparison of longitudinal loss factor for different scraper full gaps g.

g [mm]	Theory [V/pC]	Wakis [V/pC]	CST [V/pC]
3	1.935	0.892	0.974
4	1.421	0.762	0.841
5	1.026	0.628	0.696
6	0.697	—	0.555
10	~ 0	0.126	0.136

In addition to the longitudinal loss factor, the vertical transverse kick factor was evaluated. For the analytical estimate, the expression given by Zagorodnov for a rectangular collimator was used [8]:

$$k_\perp = \frac{Z_0 c}{4\sqrt{\pi}} \frac{\alpha h}{\sigma_z} \left(\frac{1}{g^2} - \frac{1}{b^2} \right), \tag{3}$$

For the numerical evaluation with Wakis, the driving beam was vertically offset by 1 mm from the chamber center in order to excite the transverse wakefield. The vertical kick factor was then extracted from the simulated vertical wake potential. The comparison between the analytical estimate and the Wakis results is summarized in Table 2.

Table 2: Vertical kick factor for different scraper full gaps. The Wakis results were obtained with a 1 mm vertical beam offset.

Gap (mm)	**Theory V/(pC·mm)**	**Wakis V/(pC·mm)**
3	1.526	1.412
4	0.9554	0.890
5	0.6568	0.613
10	0.1774	0.121

RW IMPEDANCE STUDY

The resistive wall (RW) impedance is one of the dominant broadband contributions in Elettra 2.0 due to the relatively small vertical aperture of several vacuum chambers distributed around the ring. This contribution is particularly important since the machine operates with short bunches and multiple vacuum chambers have narrow vertical dimensions, making the transverse RW contribution non-negligible. The Elettra 2.0 vacuum system consists of different chamber geometries and materials, which can be approximately grouped into four categories: **multipole chambers** with rhomboidal cross section (27 × 17 mm) made of Cu with NEG coating, **dipole chambers** with 17.7×15.4 mm aperture made of stainless steel with NEG coating, **dipole chambers with photon extraction** ports with rhomboidal cross section (27×17 mm) made of stainless steel with NEG coating, and long straight section chambers with elliptical cross section (27 × 9 mm) made of Al with NEG coating. The NEG coating thickness is 0.5 μm. The analytical RW impedance for the uncoated beam pipe was first estimated using the classical expressions for a circular resistive chamber from A. Chao [9]. The longitudinal and transverse impedances per unit length are given by

$$\frac{Z_\parallel^{(0)}(\omega)}{L} \sim \frac{1-\mathrm{sgn}(\omega)i}{2\pi b\,\delta_2\,\sigma_2} \qquad \frac{Z_\perp^{(1)}(\omega)}{L} \sim \frac{c}{\omega}\frac{1-\mathrm{sgn}(\omega)i}{\pi b^3\,\delta_2\,\sigma_2} \tag{4}$$

For chambers coated with NEG, the two-layer resistive wall model described in [10] was used. Under the condition that the coating thickness Δ is much smaller than the coating skin depth, the longitudinal and transverse impedances can be approximated as

$$\frac{Z_\parallel(\omega)}{C} \simeq \frac{Z_0\omega}{4\pi cb}\left[[\mathrm{sgn}(\omega)-i]\delta_2 - 2i\Delta\left(1-\frac{\sigma_1}{\sigma_2}\right)\right] \tag{5}$$

$$\frac{Z_\perp(\omega)}{C} \simeq \frac{Z_0}{2\pi b^3}\Big([1-i\ \mathrm{sgn}(\omega)]\delta_2 - 2i\Delta\ \mathrm{sgn}(\omega)\left(1-\frac{\sigma_1}{\sigma_2}\right)\Big) \tag{6}$$

where b is the effective beam pipe radius, ω is the angular frequency, c is the speed of light, Z_0 is the impedance of free space, σ_1 and σ_2 are the conductivities of the coating and substrate materials, respectively, Δ is the coating thickness, and δ_1 and δ_2 denote the skin depths of the coating and substrate materials, respectively. To benchmark the analytical model, the RW impedance was also evaluated using IW2D [**?**], which provides semi-analytical calculations, and CST, which performs full 3D wakefield simulations using realistic chamber geometries.

The comparison between the three methods for the total vertical kick factor and longitudinal loss factor is summarized in Table 3. The overall agreement between analytical, semi-analytical, and numerical approaches validates the RW model used in the updated Elettra 2.0 impedance budget. The increase observed in the coated case is mainly related to the additional contribution of the NEG layer.

Table 3: Comparison of total RW contribution obtained with different methods.

	Without NEG coating		
Parameter	**Theory**	**IW2D**	**CST**
Ver. kick factor [V/pC/mm]	2.68	2.36	3.19
Loss factor [V/pC]	4.31	4.34	4.69
	With NEG coating		
Parameter	**Theory**	**IW2D**	**CST**
Ver. kick factor [V/pC/mm]	3.04	2.54	4.09
Loss factor [V/pC]	4.23	4.29	5.76

BPMS IMPEDANCE STUDY

A total of 168 BPMs are foreseen for Elettra 2.0. Their electromagnetic model is shown in Figure 2. To push the first peak of the longitudinal beam coupling impedance to

higher frequencies, the pickups adopt a conical shape. For an RMS bunch length of $\sigma_{\mathrm{rms}} = 4$ mm, the corresponding wake potential and impedance are shown in Figure 3 and 4. Considering all 168 BPMs, the total longitudinal loss factor amounts to 0.27 V/pC, while the transverse kick factors are −0.34 V/(pC·mm) and −0.19 V/(pC·mm) in the horizontal and vertical planes, respectively.

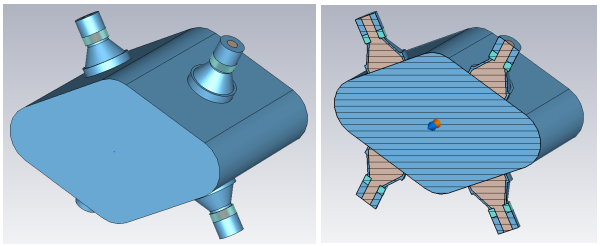

(a) (b)

Figure 2: BPM EM model.

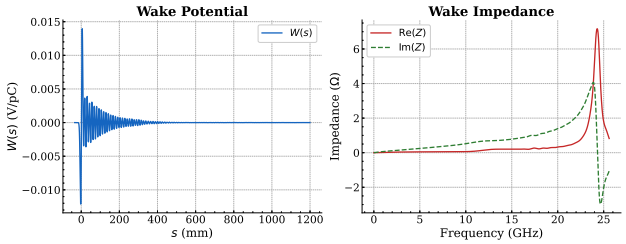

Figure 3: BPM longitudinal wake potential and beam coupling impedance.

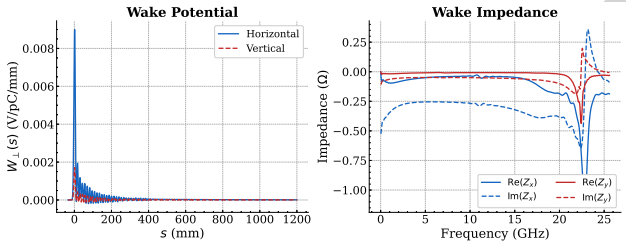

Figure 4: BPM Transverse wake potential and beam coupling impedance.

FLANGES IMPEDANCE STUDY

Owing to their large number, approximately 250 in the Elettra 2.0 storage ring, flanges require a careful assessment of their overall contribution to the machine's beam coupling impedance. Two types of flanges have been considered in the Elettra 2.0 initial design [11]. Both are characterized by a mechanical gap that interrupts the electrical continuity between the opposing sides of the vacuum pipe they are intended to join.

For each flange type, the resulting beam coupling impedance is governed by the amplitude of the mechanical gap and by the shape and volume of the (parasite) cavity located behind it. To minimize the longitudinal beam-coupling impedance, and consequently the RF heating arising from beam-induced power loss in the parasite cavity, the mechanical gap must be effectively shielded from the electromagnetic field of the beam. A straightforward yet efficient in-house solution is the development of an RF-contact gasket, whose mechanical design and mounting configuration are illustrated in Figure 5 [12]. The rhomboidal RF gasket (1) provides the electrical connection between two opposite sides of the flange, closing the gap along almost all its perimeter. The residual apertures along the RF gasket act as ports through which beam-induced electromagnetic energy can enter the parasite cavity. Due to the reduced dimensions of such apertures, the coupling between the cavity and the beam is almost negligible, as shown by the simulations reported in Figure 6.

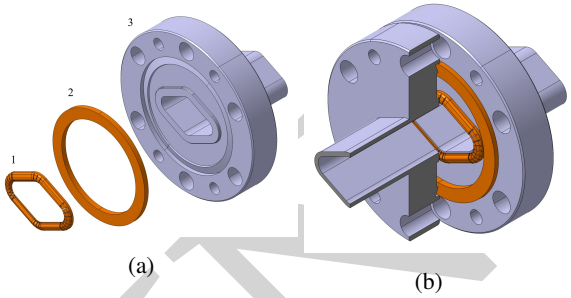

(a) (b)

Figure 5: Impedance mitigation through RF gasket: (**a**) flange assembly before mounting, RF contact gasket (1), CF vacuum gasket (2), flange (3) and (**b**) fully assembled.

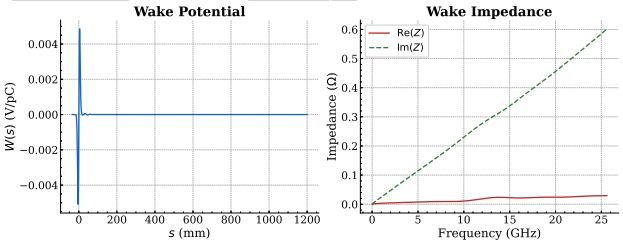

Figure 6: Flange longitudinal wake potential (**a**) and beam coupling impedance (**b**) of a flange that mounts the RF gasket.

CONCLUSION

An updated impedance budget for Elettra 2.0 has been obtained from detailed numerical simulations benchmarked against analytical and semi-analytical models. The results are overall consistent with the estimates reported in the Technical Design Report, confirming the validity and order of magnitude of the initial impedance assumptions.

The use of realistic geometries in the numerical simulations increases confidence in the impedance evaluation by providing a more faithful representation of the actual machine components and their electromagnetic interaction with the beam. Among the components studied, the RW and scraper represent the dominant contributions, while BPMs and RF-contact gasket flanges remain comparatively small. These results provide a more reliable impedance model for ongoing beam dynamics and stability studies for Elettra 2.0.

REFERENCES

[1] Elettra Sincrotrone Trieste, *Elettra 2.0 Technical Design Report*, Trieste, Italy, Nov. 2024. Available: Elettra2/TDR.pdf

[2] E. Karantzoulis *et al.*, "Design strategies and technology of Elettra 2.0 for a versatile offer to the user community," Nucl. Instrum. Methods Phys. Res. A 1060 (2024) 169007. doi:10.1016/j.nima.2023.169007

[3] L. Tosi, E. Karantzoulis, and V. Smaluk, "Measurements of the Impedance Introduced by the Vertical Scraper at ELETTRA and its Effects", in *Proc. EPAC'02*, Paris, France, Jun. 2002, paper WEPRI027, pp. 1568–1570.

[4] K. L. F. Bane, G. Stupakov, and I. Zagorodnov, "Optical approximation in the theory of geometric impedance," *Phys. Rev. ST Accel. Beams*, vol. 10, p. 054401, 2007. doi:10.1103/PhysRevSTAB.10.054401

[5] A. Blednykh and S. Krinsky, "Loss Factor of Tapered Structures for Short Bunches", in *Proc. PAC'11*, New York, NY, USA, Mar.-Apr. 2011, paper WEP176, pp. 1816–1818.

[6] E. de la Fuente Garcia *et al.*, "WAKIS", Zenodo, 2025. doi:10.5281/zenodo.15527405

[7] Dassault Systèmes, *CST Studio Suite*, cst-studio-suite

[8] A. M. Toader and R. J. Barlow, "Comparison of Collimator Wakefields Formulae", in *Proc. EPAC'08*, Genoa, Italy, Jun. 2008, paper WEPP166, pp. 2877–2879.

[9] A. W. Chao, *Physics of Collective Beam Instabilities in High Energy Accelerators*, John Wiley & Sons, New York, 1993.

[10] M. Migliorati, E. Belli, and M. Zobov, "Impact of the resistive wall impedance on beam dynamics in the Future Circular e^+e^- Collider," *Phys. Rev. Accel. Beams*, vol. 21, p. 041001, 2018. doi:10.1103/PhysRevAccelBeams.21.041001
"IW2D: Impedance and Wakefield in 2D". https://gitlab.cern.ch/IRIS/IW2D

[11] S. Cleva, I. Cudin, L. Rumiz, E. Karantzoulis, A. Passarelli, and M. Comisso, "Beam coupling impedance contribution of flange aperture gaps: a numerical study for Elettra 2.0", in *Proc. IPAC'23*, Venice, Italy, May 2023, pp. 3446–3449. doi:10.18429/JACoW-IPAC2023-WEPL146

[12] I. Mrak, G. Scrimali and S. Cleva, "Flange aperture gap RF contact gasket for Elettra 2.0 storage ring", in *Proc. MEDSI2025*, Lund, Sweden, Sep. 2025, pp. 220-223. doi:10.18429/JACoW-MEDSI2025-WEP31